

Characterization of PARIS LaBr₃(Ce)-NaI(Tl) phoswich detectors upto $E_\gamma \sim 22$ MeV

C. Ghosh^a, V. Nanal^{a*}, R.G. Pillay^a, Anoop K.V.^b, N. Dokania^c, Sanjoy Pal^b, M.S. Pose^a, G. Mishra^d, P.C. Rout^d, Suresh Kumar^d, Deepak Pandit^e, Debasish Mondal^e, Surajit Pal^e, S.R. Banerjee^e, Paweł J. Napiorkowski^f, Oliver Dorvaux^g, S. Kihel^g, C. Mathieu^g, A. Maj^h

^aDepartment of Nuclear and Atomic Physics, Tata Institute of Fundamental Research, Homi Bhabha Road, Mumbai 400 005, India.

^bPelletron Linac Facility, Tata Institute of Fundamental Research, Homi Bhabha Road, Mumbai 400 005, India.

^cIndia-based Neutrino Observatory, Tata Institute of Fundamental Research, Homi Bhabha Road, Mumbai 400 005, India.

^dNuclear Physics Division, Bhabha Atomic Research Centre, Trombay, Mumbai 400 085, India.

^eVariable Energy Cyclotron Centre, 1/AF-Bidhannagar, Kolkata 700 064, India.

^fHeavy Ion Laboratory, University of Warsaw, Pasteura 5a, 02-093 Warsaw, Poland.

^gInstitut Pluridisciplinaire Hubert Curien, UNISTRA, CNRS, rue du Loess, 67200 Strasbourg, France.

^hThe Niewodniczański Institute of Nuclear Physics, Polish Academy of Sciences, ul. Radzikowskiego 152, 31-342 Kraków, Poland.

E-mail: nanal@tifr.res.in

ABSTRACT: In order to understand the performance of the PARIS (Photon Array for the studies with Radioactive Ion and Stable beams) detector, detailed characterization of two individual phoswich (LaBr₃(Ce)-NaI(Tl)) elements has been carried out. The detector response is investigated over a wide range of $E_\gamma = 0.6$ to 22.6 MeV using radioactive sources and employing $^{11}\text{B}(p, \gamma)$ reaction at $E_p = 163$ keV and $E_p = 7.2$ MeV. The linearity of energy response of the LaBr₃(Ce) detector is tested upto 22.6 MeV using three different voltage dividers. The data acquisition system using CAEN digitizers is set up and optimized to get the best energy and time resolution. The energy resolution of $\sim 2.1\%$ at $E_\gamma = 22.6$ MeV is measured for the configuration giving best linearity upto high energy. Time resolution of the phoswich detector is measured with a ^{60}Co source after implementing CFD algorithm for the digitized pulses and is found to be excellent (FWHM ~ 315 ps). In order to study the effect of count rate on detectors, the centroid position and width of the $E_\gamma = 835$ keV peak were measured upto 220 kHz count rate. The measured efficiency data with radioactive sources are in good agreement with GEANT4 based simulations. The total energy spectrum after the add-back of energy signals in phoswich components is also presented.

KEYWORDS: Gamma detectors, Digital signal processing (DSP).

Contents

1. Introduction	1
2. Experimental Details	2
3. Linearity and Count Rate Effects	5
3.1 Linearity of Energy Response	5
3.2 Detector Gain Stability as a Function of Count Rate	7
4. Analysis of Detector Response	8
4.1 Energy Resolution	9
4.2 Time Resolution	12
4.3 Efficiency	12
4.4 Total Energy Spectrum	13
5. Summary and Conclusions	15

1. Introduction

Scintillation detectors are widely used in Nuclear and Particle Physics research due to their good time resolution, high efficiency and moderate energy resolution. In recent years, rare-earth halide based scintillators ($\text{LaBr}_3(\text{Ce})$, $\text{LaCl}_3(\text{Ce})$, CeBr_3) have found attractive applications [1–8] due to their excellent energy resolution ($\leq 4\%$ at 662 keV), sub-nanosecond time resolution and relatively higher intrinsic efficiency as compared to the conventional scintillators such as $\text{NaI}(\text{Tl})$ and BaF_2 . Amongst these novel scintillators, the $\text{LaBr}_3(\text{Ce})$ detector has the best energy resolution [9] and offers a possible alternative for high resolution gamma ray spectroscopy, particularly for experiments with exotic beams and low-multiplicity events.

The PARIS (Photon Array for the studies with Radioactive Ion and Stable beams) detector, a high efficiency gamma-calorimeter comprising $\text{LaBr}_3(\text{Ce})$ - $\text{NaI}(\text{Tl})$ phoswich elements (manufactured by Saint-Gobain Crystals), is being developed for the measurement of high energy gamma rays [10, 11]. The array consists of multiple clusters, each in turn being made of 9 (3×3) phoswich elements. The individual phoswich detector element consists of a front $\text{LaBr}_3(\text{Ce})$ crystal ($2'' \times 2'' \times 2''$) optically coupled to a $\text{NaI}(\text{Tl})$ crystal ($2'' \times 2'' \times 6''$) at the back. Both these crystals are encapsulated together with a single optical window at the rear end, which is coupled to a 8 stage, 46 mm diameter Hamamatsu photomultiplier tube (PMT) R7723-100 [12–14]. This PMT with the maximum sensitivity at $\lambda \sim 420$ nm and a fast pulse rise time ~ 1.7 ns is well suited for both $\text{LaBr}_3(\text{Ce})$ ($\lambda_{\text{max}} \sim 380$ nm) and $\text{NaI}(\text{Tl})$ ($\lambda_{\text{max}} \sim 415$ nm). The signals from the $\text{LaBr}_3(\text{Ce})$ and

*Corresponding author.

NaI(Tl) can be easily resolved due to their widely different decay times, namely, 16 ns and 250 ns, respectively. Ziebliński *et. al.* [14] have demonstrated the feasibility of separation of individual components with both analog and digital signal processing upto $E_\gamma = 6.13$ MeV. They have also shown that good energy resolution can be obtained by adding the LaBr₃(Ce) and NaI(Tl) signals.

It should be mentioned that most of the measurements for characterization of LaBr₃(Ce) detectors of different sizes are done with various radioactive sources and hence are restricted to low energy gamma rays. A few high energy measurements, by studying gamma rays with (p, γ) reactions, have been reported [2,4,5]. It is well known that the intense light yield of LaBr₃(Ce) crystal (63 photon/keV γ [9]) may saturate the response of PMT and consequently leads to the non-linearity in energy calibration of the detector. To achieve better linearity over a broad energy range, an active voltage divider has been employed [2,5]. Ciemała *et al.* [4] have studied the response of a cylindrical LaBr₃(Ce) (2'' length, 2'' dia) which is similar to the LaBr₃(Ce) crystal in the phoswich detector element. They have reported energy resolution of 0.7% and intrinsic photo-peak efficiency of about 0.65% at 17.6 MeV. They also observed $\sim 10\%$ non-linearity at this energy. It should be pointed out that for the PARIS detector, the response is further complicated due to the composite nature of the detector and it is important to understand how the performance of the LaBr₃(Ce) is modified by coupling to NaI(Tl). Preliminary high energy gamma ray spectra ($E_\gamma = 22.6$ MeV) of the phoswich detector using analog signal processing in $^{11}\text{B}(p, \gamma)$ reaction were reported in Ref. [14], which also showed a significant non-linearity. Since the readout is common to both LaBr₃(Ce) and NaI(Tl), the optimization for linearity in LaBr₃(Ce) can significantly affect the NaI(Tl) output. In order to address these issues, a detailed characterization of two phoswich elements have been performed over a wide energy range (0.6 – 22.6 MeV). Given the composite nature of the pulse, digital processing is best suited for the phoswich detector. In the present study, the acquisition system using CAEN digitizers (12 bit 250 MS/s, 10 bit 1 GS/s) [15] is optimized to get the best energy and time resolution. The energy resolution is extracted by fitting the observed lineshape to the simulated energy spectrum generated using GEANT4 [16]. This paper reports the study of the linearity, detector gain stability for high count rates, energy resolution, efficiency and time resolution for the phoswich detector. The total energy spectrum after the add-back of energy signals in phoswich components is presented for high energy gamma rays in $^{11}\text{B}(p, \gamma)$ reaction.

2. Experimental Details

Two phoswich detectors D1 and D2 were coupled to PMT1 and PMT2, respectively, with optical grease. The ORTEC model 556 unit (with regulation $\leq 0.0025\%$, temperature instability $< \pm 50$ ppm/ $^\circ\text{C}$, long term drift $< 0.03\%/24\text{-hour}$) was used for high voltage bias. Measurements were carried out with various radioactive sources and the radiative proton capture reaction $^{11}\text{B}(p, \gamma)$. Details of gamma ray energies are given in Table 1 and Table 2. The high energy gamma rays were studied in two separate experiments - first using the 163 keV proton beam from the ECR source [17] and second using the 7.2 MeV proton beam from the Pelletron Linac Facility, Mumbai [18]. Figure 1 shows a picture of the experimental set-up used in the radiative capture reactions. A thin walled, compact Aluminum chamber was used and the detectors were placed at $+45^\circ$ and -45° with respect to the beam direction at about 6 cm from the target. The natural Boron target (~ 1 mg/cm²) was made by electro-deposition on a 127 μm thick Tantalum backing. Due to the thick backing

the total incident proton charge on the target could not be measured and hence absolute efficiency could not be deduced for high energy gamma rays. Typical current used in the reaction at $E_p = 163$ keV was $\sim 2 \mu\text{A}$ while that at $E_p = 7.2$ MeV was about ~ 10 nA. A thin Lead absorber (~ 3 mm) was kept in front of both the detectors to absorb X-rays and low energy gamma rays. Adequate shielding was provided to reduce the neutron background in the experiment with $E_p = 7.2$ MeV. Measurements were carried out over an extended period of time and the detector performance was periodically monitored.

Table 1. Radioactive sources used for measurements together with E_γ [19] and source strengths N_s (as on 1st Feb. 2015).

Source	E_γ (MeV)	N_s (Bq)
^{22}Na	0.511, 1.2748	–
^{137}Cs	0.6617	13738 (427)
^{54}Mn	0.8348	8260 (298)
^{60}Co	1.1732, 1.3325	9846 (276)
$^{241}\text{Am} - ^9\text{Be}$	4.439	9625 (147)
$^{239}\text{Pu} - ^{13}\text{C}$	6.130	–

Table 2. Radiative capture reactions and emitted E_γ [20]

Reaction	E_p (MeV)	E_γ (MeV)
$^{11}\text{B}(p, \gamma)$	0.163	4.439, 11.680
$^{11}\text{B}(p, \gamma)$	7.2	4.439, 5.020, 18.118, 22.557

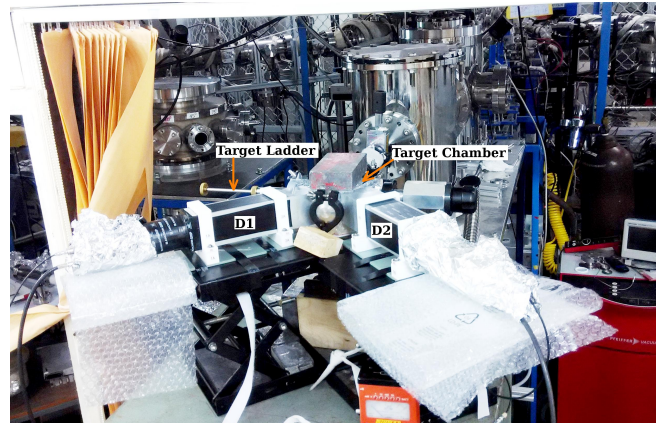


Figure 1. (Color online) The experimental set-up used for radiative proton capture reactions.

As mentioned earlier, for composite pulse from the phoswich detector, the digital signal processing is an ideal choice. However, both analog and digital data acquisition systems were used for part of the measurements ($^{11}\text{B}(p, \gamma)$ at $E_p = 163$ keV) for comparison. The analog electronics set-up

comprised two charge sensitive ADCs (Silena 4418/Q) with a short gate of 300 ns (for $\text{LaBr}_3(\text{Ce})$ signal) and a long gate of 900 ns (for both $\text{LaBr}_3(\text{Ce})$ and $\text{NaI}(\text{Tl})$ signals) and data was acquired with LAMPS [21], a CAMAC-based acquisition and analysis software, similar to preliminary work reported in Ref. [14].

Two CAEN make VME based digitizers V1720e (12 bit - 250 MS/s, 2 Volt dynamic range) and V1751 (10 bit - 1 GS/s, 1 Volt dynamic range) were used to digitize and process the detector pulse [15]. The WAVEDUMP software permits the recording of entire pulse after digitization with settable pre-trigger length. Typical pulses recorded with V1720e for high energy gamma rays corresponding to different interaction points inside the detector are shown in Fig. 2. The clear separation of events corresponding to full energy deposition in $\text{LaBr}_3(\text{Ce})$ or $\text{NaI}(\text{Tl})$ as well as partial energy in either of them, is evident. An online algorithm implementing constant fraction discrimination has been developed for timing measurements from the digitized pulse.

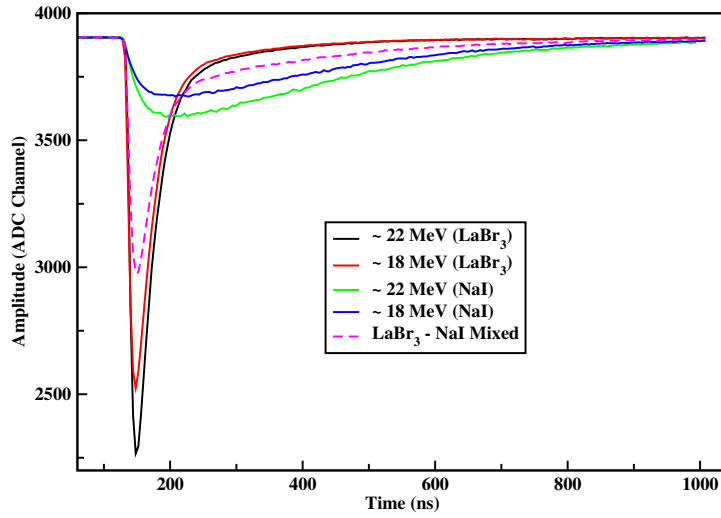


Figure 2. (Color online) High energy gamma ray pulses in detector D1 recorded with V1720e (250 MS/s) digitizer using wavedump software. The mixed signal shown corresponds to an arbitrary E_γ between 18 and 22 MeV. The baseline is set at an arbitrary value around 3900.

The DPP-PSD firmware, enables the integration of the digitized pulse over two different pre-settable time windows, which are recorded together with the time stamp (in units of the sampling frequency) for every event. The recorded data is converted into ROOT [22] format for further processing. The short and long gate widths have been optimized to get the best energy resolution at 4.4 MeV and found to be 300 ns and 900 ns, respectively. A typical 2D histogram of Q_{short} and Q_{long} , integrated charges over short and long time gates, respectively (approximately corresponding to E_{LaBr_3} and E_{total}) obtained in $^{11}\text{B}(p, \gamma)$ reaction at $E_p = 163$ keV is shown in Fig. 3 for the D2 detector. The $\text{LaBr}_3(\text{Ce})$ and $\text{NaI}(\text{Tl})$ spectra are constructed by appropriate projections of this spectrum. The projected spectra are analyzed using peak fitting routines in LAMPS and ROOT.

For studying the linearity of the energy response of the detector, the bias voltage for the PMT R7723-100 ($V_{\text{max}} = -2$ kV) was varied from -1.0 kV to -1.8 kV. It should be noted that at low PMT voltage, the signal from the $\text{NaI}(\text{Tl})$ was very poor and the threshold setting was limited by the 12 bit ADC. Further, in order to disentangle the detector and the PMT + base (i.e., voltage divider

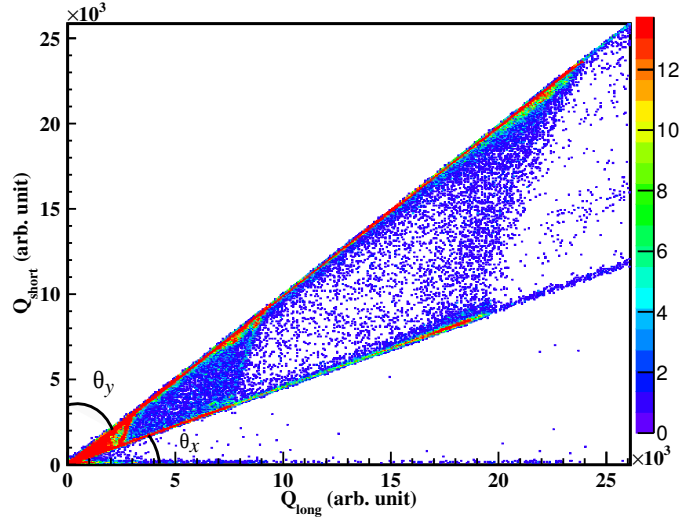


Figure 3. (Color online) A two dimensional histogram (Q_{short} vs Q_{long}) constructed from the data acquired with DPP-PSD firmware in $^{11}\text{B}(p, \gamma)$ reaction at $E_p = 163$ keV, for D2 detector. The angles θ_x and θ_y represent the tilt angles for pure events in NaI(Tl) and LaBr₃(Ce) crystals with respect to Q_{long} and Q_{short} axis, respectively.

circuit) set contribution, some measurements were repeated by interchanging these combinations, viz., D1 + PMT1, D2 + PMT2 and D1 + PMT2, D2 + PMT1. The effects due to temperature variations are expected to be negligible and not considered in the present study, since the ambient temperature was stable within $\pm 1^\circ\text{C}$. The long term stability of the detectors was tested and found to be better than 1% over a period of 24 hours.

3. Linearity and Count Rate Effects

3.1 Linearity of Energy Response

As mentioned in the earlier section, one of the major concerns for LaBr₃(Ce) detector is the non-linearity of the detector response at high energy owing to its high light yield. A total of three types of the voltage divider circuits were used in the measurements, namely, B1 – the standard Hamamatsu make resistive voltage divider E5859-15, B2 – a simple modification from the B1 with the gain of first two dynode stages reduced to half of the original values and B3 – a passive voltage divider developed by IPHC Strasbourg group for the PARIS detector [23]. The standard configuration for the dividers uses charge pump capacitors only at the last few gain stages. However, in order to handle larger signals arising from the LaBr₃(Ce) elements and higher counting rates, the modified divider uses charge pump capacitors at all stages with higher value capacitors than in standard configurations. The raw pulse heights from the two detectors are different, mainly due to PMT + voltage divider combination. Initially, for comparative study of three voltage dividers, the same high voltage was applied and hence the pulse heights were different for different voltage dividers. For linearity and count rate studies with B3 voltage divider, the high voltage was adjusted to get the similar pulse height from the two detectors to ensure similar PMT chain current. The

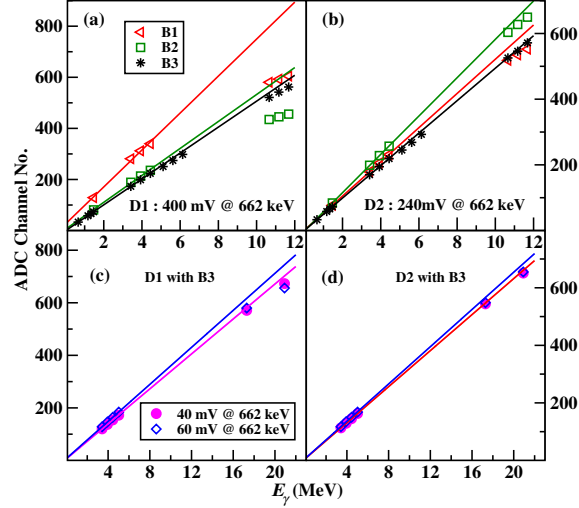


Figure 4. (Color online) Energy response linearity for $\text{LaBr}_3(\text{Ce})$ in phoswich detector : (a) for D1 with different voltage dividers upto $E_\gamma = 11.7$ MeV; (b) same as (a) for D2; (c) for D1 with B3 voltage divider and upto $E_\gamma = 22.6$ MeV at two different applied voltages, (d) same as (c) for D2. The symbols represent the measured data, while the straight lines are the extrapolation of linear calibration using gamma ray energies up to 4.4 MeV.

detector signals were suitably attenuated using a passive attenuator to make it acceptable for the ADC input range and to adjust the full energy scale to ~ 17 MeV and 25 MeV for the radiative capture reactions at $E_p = 163$ keV and 7.2 MeV, respectively. The energy responses of the detectors were found to be linear upto 4.4 MeV for all the voltage dividers upto the bias voltage of ~ 1.8 kV. Fig. 4(a) - (b) show the comparison of energy response with different voltage dividers upto $E_\gamma = 11.7$ MeV for D1 and D2, respectively. Non-linearity (α) of the energy response is estimated as the percentage deviation from the linear extrapolation of energy calibration upto 4.4 MeV. Table 3 gives the measured non-linearity for different voltage dividers with same high voltage together with the anode pulse height (A1) for 662 keV gamma ray. The detector D1 having larger pulse height, shows higher non-linearity as expected.

Table 3. The non-linearity (α) of the $\text{LaBr}_3(\text{Ce})$ detector with different voltage dividers (B1, B2, B3) at $E_\gamma = 11.7$ MeV. The anode pulse height (A1) for 662 keV in the $\text{LaBr}_3(\text{Ce})$ crystal is also listed ($V_{D1} = -1.6$ kV and $V_{D2} = -1.8$ kV).

Detector	B1		B2		B3	
	A1 (V)	α (%)	A1 (V)	α (%)	A1 (V)	α (%)
D1	1.5	31	1.3	27	0.4	5
D2	0.68	9	0.6	5	0.24	1

It is evident that the B3 type voltage divider is significantly better even at $E_\gamma \sim 12$ MeV. Therefore, linearity upto 22.6 MeV was investigated only for B3 type divider for A1 ~ 40 mV ($V_{D1} = -1.040$ kV and $V_{D2} = -1.310$ kV) and 60 mV ($V_{D1} = -1.123$ kV and $V_{D2} = -1.418$ kV). The energy range ($E_{\text{full-scale}}$) was adjusted to ~ 30 MeV with suitable attenuation. The results are

Table 4. The non-linearity (α) of the LaBr₃(Ce) detector with B3 type voltage divider at $E_\gamma = 18.1$ and 22.6 MeV for different high voltages (A1) has same meaning as in Table 3.

Detector	Non-linearity (%)			
	$E_\gamma = 18.1$ MeV		$E_\gamma = 22.6$ MeV	
	A1=60 (mV)	A1=40 (mV)	A1=60 (mV)	A1=40 (mV)
D1	6	2	12	4
D2	3	1	4	2

shown in Fig. 4 (c) - (d) and tabulated in Table 4. It should be mentioned that the centroid for 18.1 and 22.6 MeV gamma rays were obtained from the simulated spectra after folding the resolution function, as described in the later section.

For both detectors, at A1 \sim 40 mV setting the non-linearity is about 2–4% at $E_\gamma = 22.6$ MeV. However, it should be noted that the bias voltage is significantly lower (~ -1.0 to -1.3 kV), which impacts both energy and time resolution. Hence A1 \sim 60 mV, which yields $\alpha \sim 10\%$, would be an optimum choice. In case of NaI(Tl), the observed non-linearity in all of the above configurations was smaller than 1% upto $E_\gamma \sim 11.7$ MeV.

3.2 Detector Gain Stability as a Function of Count Rate

Considering excellent time resolution of the LaBr₃(Ce) detector, it is envisaged that the PARIS detector will be used in a close geometry thereby enhancing the detection efficiency. Thus, high count rate handling capability is essential. Generally, during in-beam experiment any variations in beam intensity can lead to fluctuations in count rate. Given the fact that the phoswich detector pulse has a width of about $\sim 1 \mu\text{s}$, in principle the detector has a large count rate handling capacity (\sim MHz). However, if the phoswich detector + PMT + voltage divider assembly is not robust with respect to the count rate variations, it will result in the degradation of the energy resolution. At high count rate, a combination of pile-up and variation in the PMT gain comes into effect and the peak shift will depend on the dominance of these two effects.

To estimate the robustness of phoswich detector + PMT for count rate variation, the centroid drift and the resolution of 835 keV gamma ray (from ⁵⁴Mn source) in the LaBr₃(Ce) were studied over a broad count rate range of 2 - 220 kHz. This was achieved by keeping a weak ⁵⁴Mn source (8.3 mBq) at a fixed distance from the detector and by varying the position of a strong ¹³⁷Cs source (4 MBq). The choice of the low energy ($E_\gamma = 662$ keV) strong source ensured that the centroid of 835 keV gamma ray line was minimally affected due to pile-up, summing and Compton edge from the strong source. A stabilization time of ~ 30 min was allowed for each setting. The drift in centroid for each detector was measured with respect to the lowest count rate (2 kHz). Fig. 5 shows variation in peak centroid and FWHM for D1 (panels (a) - (b)) and for D2 (panels (c) - (d)) with both PMT bases having the B3 type divider. Data correspond to different high voltages and the respective anode pulse heights (A1) for 662 keV gamma ray are mentioned in the legends.

At the lowest voltage (A1 = 40 mV), the centroid shift for D1 is less than 1.5% (11 keV) even at the highest count rate of 220 kHz, while the FWHM worsens by $\sim 13\%$ (~ 5 keV). At the highest count rate, errors in FWHM are larger due to fitting errors. The shifts at high count

rate are expectedly worse (centroid shift $\sim 5\%$) for higher pulse heights ($A1 = 140$ mV). It may be noted that overall the shifts are smaller for D2 as compared to the D1. As it is evident from the Fig. 5, the shifts in the centroid of D1 and D2 are in the opposite direction. By interchanging the PMT + base sets on two detectors (i.e. with D1 + PMT2 and D2 + PMT1), it was verified that the count rate effects are intrinsic to the PMT + voltage divider combination. It should be mentioned that larger count rate variation at 220 kHz (centroid shift $\sim 3.7\%$ i.e. 31 keV for $A1 = 40$ mV) was observed with Wiener EHSF020n (16 - channel, 2 kV, 4 mA) high voltage supply. It is clear that the performance of the detectors is quite stable in the range 50 to 150 kHz in the region of interest ($A1 = 40$ to 140 mV).

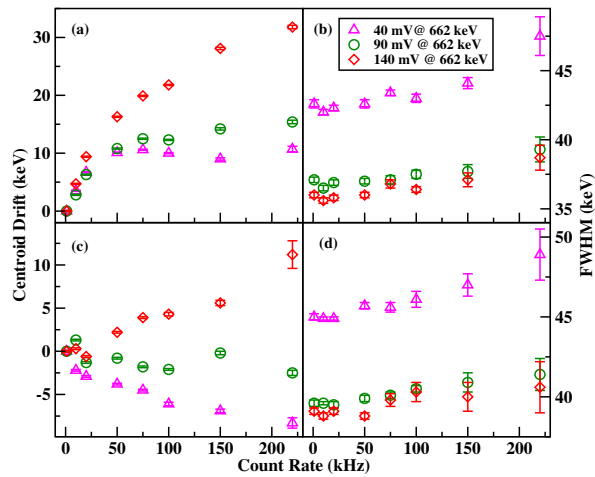


Figure 5. (Color online) Variation of the centroid shift and FWHM of 835 keV gamma ray peak in $\text{LaBr}_3(\text{Ce})$ as a function of count rate (a) and (b) for D1 detector; (c) and (d) for D2 detector. Measurements were done using B3 type voltage divider for different high voltages and corresponding pulse heights ($A1$) for 662 keV are listed in legends.

The count rate handling capability was also tested with the standard base B1 (90 mV @ 662 keV) and results are shown in Fig. 6. It can be seen that even at 10 kHz, the centroid shift (~ 3.7 keV) with the B1 voltage divider is significantly larger than that for the B3 (~ 1.3 keV). A similar behavior is seen for the FWHM. Hence, it is evident that performance of the B3 voltage divider is better in terms of linearity and stability against count rate variation.

4. Analysis of Detector Response

The phoswich detector response is simulated using GEANT4.10 [16]. Detector geometry as per design is employed including 1 mm thick Aluminum cover but the optical window is not considered. The source geometry is taken to be point like for reaction measurements and most of the sources. In the case of a sealed Am-Be source, the SS capsule is incorporated in the simulation and the source is assumed to be uniformly distributed within the capsule. The Aluminum vacuum chamber and the Lead absorber are included for high energy gamma rays. Typically, 10^8 events are generated for each simulation set. The simulated spectra have been analyzed in the ROOT in a manner identical to experimental data.

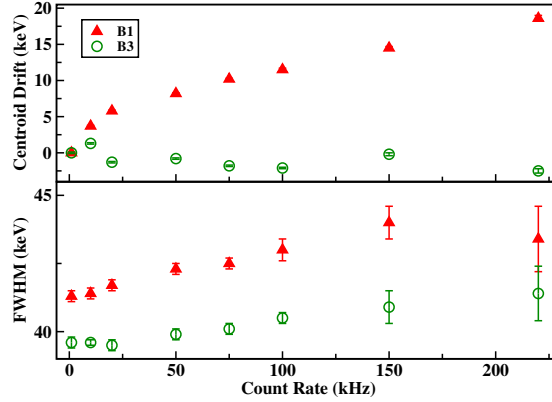


Figure 6. (Color online) Variation of the centroid shift and FWHM of 835 keV gamma ray peak as a function of count rate for D2 detector with B1 and B3 type voltage dividers for pulse height at 662 keV, A1 = 90 mV.

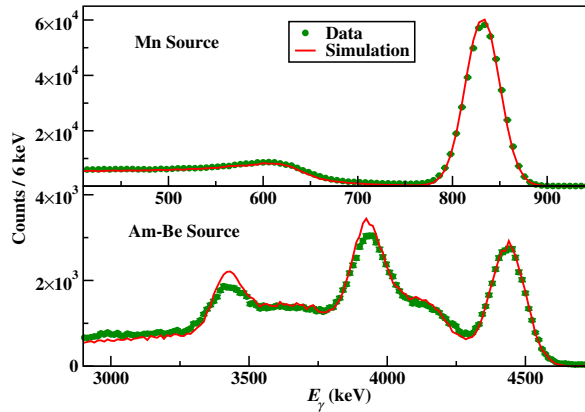


Figure 7. A Comparison of simulated (after incorporating the resolution) and experimental spectra for 835 keV and 4.4 MeV without any normalisation.

In the present work, energy resolution is studied separately for both LaBr₃(Ce) and NaI(Tl) segments. Given the nature of phoswich detector, majority of the low energy gamma rays will have primary interaction in the LaBr₃(Ce) segment. Hence, efficiency of the LaBr₃(Ce) is measured for low energy gamma rays at a distance of 10–20 cm, corresponding to a typical PARIS cluster configuration and compared with simulations. The energy resolution and efficiency at high energies are deduced from a comparison of the experimental spectra with simulated spectra.

A comparison of the simulated and the background corrected experimental spectra for 835 keV and 4.4 MeV gamma rays for D1-LaBr₃(Ce) detector is shown in Fig. 7 on an absolute scale, after folding the resolution of 5.1% for 835 keV and 3.3% for 4.4 MeV. The excellent agreement between simulations and data for complete line shape including escape peaks for the 4.4 MeV is evident.

4.1 Energy Resolution

For low energy gamma rays ($E_\gamma < 4.4$ MeV), the energy resolution for LaBr₃(Ce) was obtained by

a simple gaussian fit to the observed photo-peak. This was then fitted to the following equation [4]

$$FWHM/E_\gamma(\%) = \sqrt{a + b/E_\gamma}. \quad (4.1)$$

The simulated data is folded with a Gaussian resolution function, where the FWHM is given by Eq. (4.1). Then both the parameters (a, b) were varied to reproduce the experimentally observed lineshape over a wider energy range (662 keV - 22.6 MeV) for each detector. Doppler correction for $E_p = 7.2$ MeV (relative recoil velocity, $\beta_{recoil} = 0.01$) was incorporated in the simulations for gamma rays emitted in the reaction, while that for $E_p = 163$ keV is neglected as $\beta_{recoil} = 0.002$ is very small. Figure 8 shows the spectrum for 4.4 MeV gamma ray from the source and from the $^{11}\text{B}(p, \gamma)$ reaction at $E_p = 163$ keV. The effect due to Doppler broadening in the Am-Be source spectrum [24] is clearly visible and also re-emphasizes excellent energy resolution of the $\text{LaBr}_3(\text{Ce})$, even in the phoswich configuration.

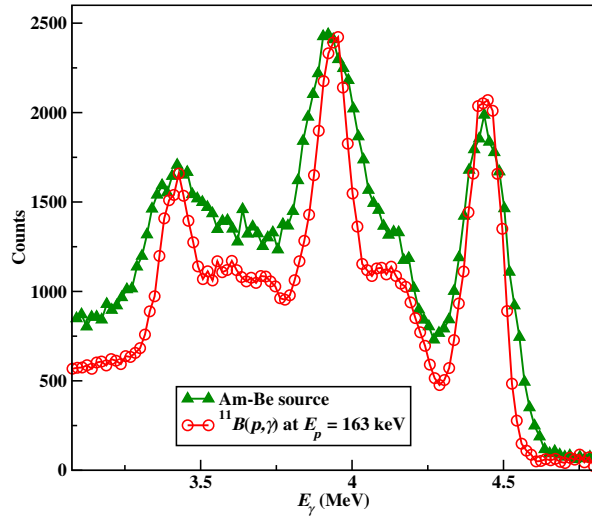


Figure 8. (Color online) Measured spectrum in D1- $\text{LaBr}_3(\text{Ce})$ for 4.4 MeV gamma ray from Am-Be source (FWHM $\sim 3.6\%$) and from $^{11}\text{B}(p, \gamma)$ reaction at $E_p = 163$ keV (FWHM $\sim 2.7\%$).

Figure 9 shows the spectra of 4.4 MeV, 11.7 MeV, 18.1 MeV and 22.6 MeV gamma rays from $^{11}\text{B}(p, \gamma)$ reaction together with simulated spectra (after folding with resolution function). Since the proton charge could not be measured, simulated spectra are normalized to area under the the photo-peak for $E_\gamma = 4.4$ MeV. For high energy gamma rays (viz., 11.7 and 22.6 MeV), spectra are normalized to the integral counts in energy range covering the 2^{nd} escape-peak to the photo-peak. Relative intensity of $E_\gamma = 18.1$ MeV with respect to $E_\gamma = 22.6$ MeV is taken to be 0.24 for the best fit to the data (Ref. value is 0.25 [27]). It can be seen that in the low energy proton reaction ($E_p = 163$ keV), where no additional background is present, excellent agreement is observed between simulation and data. In the high energy proton induced reaction ($E_p = 7.2$ MeV), the peak shapes for 18.1 and 22.6 MeV gamma rays are well reproduced but in the experimental spectra there is an excess left tail. This could be due to beam induced gamma/neutron background and neutron capture reactions in Lanthanum, Bromine and Iodine.

Figure 10 shows the energy resolution of the $\text{LaBr}_3(\text{Ce})$ segment (top panel) as a function of gamma ray energy from 0.6 to 12 MeV for the D2 detector ($A1 = 60$ mV). The symbols correspond

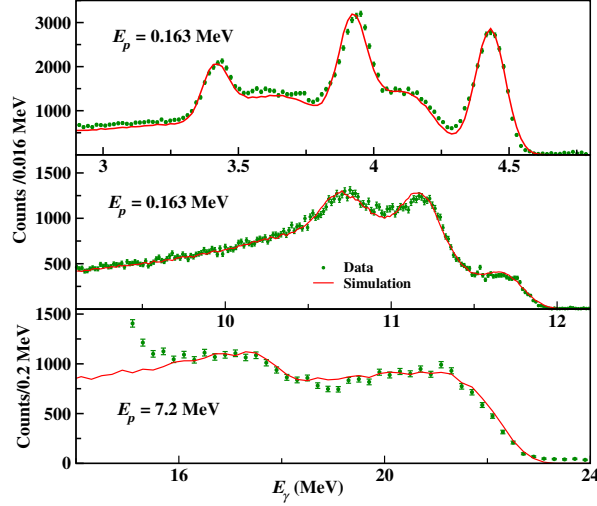


Figure 9. (Color online) Experimental spectra (solid circle) for different gamma rays together with the simulated spectrum (line) after folding in resolution function (see text).

to the data and the lines represent the fit function (Eq. (4.1)). The observed energy resolution of D1 (D2) detector shows a small improvement from 2.9 (2.8)% to 2.5 (2.3)% for $E_\gamma = 4.4$ and 11.7 MeV, respectively. The energy resolution for NaI segment, which could be fitted to a simple $1/\sqrt{E_\gamma}$ function, is shown in the bottom panel. In the case of $E_p = 7.2$ MeV induced reaction, the PMT was operated at lower voltages ($A1 = 40$ mV) to minimize non-linearity. As a result, low energy peaks (662 - 1332 keV) could not be cleanly measured. Further, the 4.4 MeV (from both Carbon and Boron) and 5.02 MeV gamma rays (from Boron) cannot be separated. Hence, the fit to resolution function was obtained using fewer points. In this configuration, the energy resolution obtained for both detectors was around $\sim 2.1\%$ at 22.6 MeV.

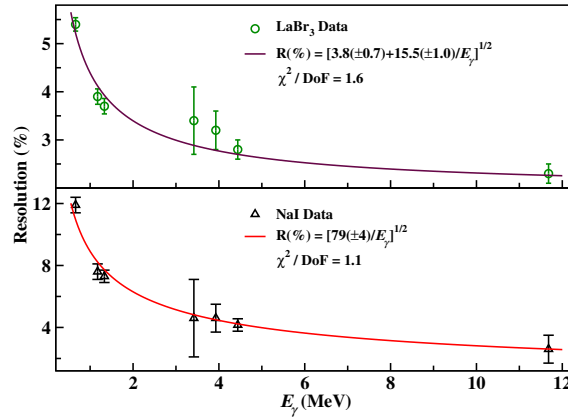


Figure 10. (Color online) Energy resolution of LaBr₃(Ce) (top) and NaI(Tl) (bottom) crystal of D2 detector up to 12 MeV ($A1 = 60$ mV). The symbols represent the measured resolution and the solid lines represent the fitted function.

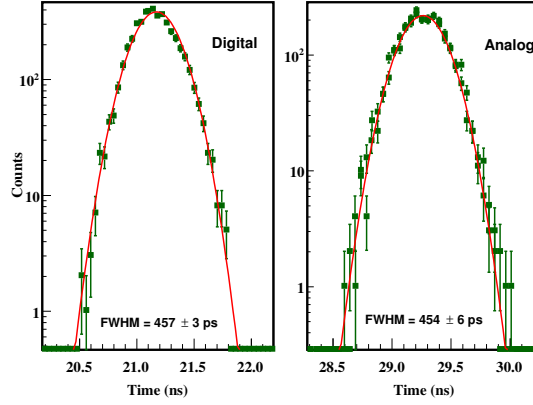


Figure 11. (Color online) Energy gated time-of-flight spectra of two $\text{LaBr}_3(\text{Ce})$ crystals of D1 and D2 using ^{60}Co source with V1751 (1 GS/s) digitizer (left panel) and with conventional analog electronics (right panel). The red line represents the gaussian fit to the experimental data.

4.2 Time Resolution

To extract timing information with a better accuracy, an algorithm implementing constant fraction discrimination with delay of 6 ns ($\sim 67\%$ of the rise-time) and 20% fraction has been developed and incorporated in the online WAVEDUMP acquisition software [28]. Linear interpolation was used to calculate the zero-crossing of the CFD pulse. Measurements were carried out with detectors D1 ($V_{D1} = -1.6$ kV) and D2 ($V_{D2} = -1.8$ kV) placed at 180 degree facing each other, with the ^{60}Co source mounted at the center at ~ 2 cm from either detector. The detector pulses were sampled with V1751 (1 GS/s) digitizer and Q_{short} , Q_{long} and T_{fine} (obtained with CFD) were stored. The left panel of Fig. 11 shows the energy gated time-of-flight (TOF) spectra of two detectors (i.e. 1173 or 1332 keV photo-peak in either $\text{LaBr}_3(\text{Ce})$ crystals). The right panel shows the time spectrum obtained using the conventional analog electronics consisting of a CFD and TAC. It can be seen that FWHM (digital) $\sim 457 \pm 3$ ps is similar to FWHM (analog) $\sim 454 \pm 6$ ps. Using an additional CeBr_3 detector, the time resolution of individual $\text{LaBr}_3(\text{Ce})$ crystal was measured to be FWHM (D1) ~ 323 ps and FWHM (D2) ~ 309 ps.

It should be noted that the above configuration corresponds to a dynamic energy scale of ~ 2 MeV in both detectors. The time resolution of the detectors was also measured at lower operating voltages ($A1 = 60$ mV) and was found to worsen by about 12% (FWHM $\sim 513 \pm 3$ ps), which is still excellent for the neutron- γ separation by TOF measurement at close distances.

4.3 Efficiency

The photo-peak efficiencies of the $\text{LaBr}_3(\text{Ce})$ crystal of D1 and D2 were measured for $E_\gamma = 662$ keV to 4.4 MeV at varying distances of 10, 15 and 20 cm from the face of the detector. The results are shown in Fig. 12 along with the simulations for 10 and 20 cm. The measured data agree with simulations at all distances. The efficiency of $\text{LaBr}_3(\text{Ce})$ crystal was also measured by keeping the source at a distance of 10 cm from the side of the detector and were found to be consistent. As mentioned earlier the intrinsic efficiency at high energy could not be extracted. However, the 4.4 MeV

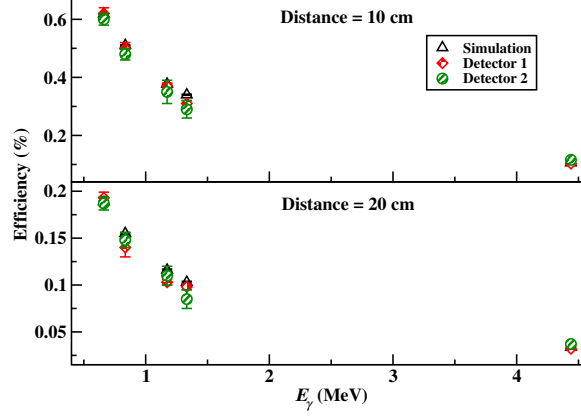


Figure 12. (Color online) The measured and simulated photo-peak efficiency of the $\text{LaBr}_3(\text{Ce})$ crystals of D1 and D2 at a distance of 10 and 20 cm from the face of the detector.

and 11.7 MeV gamma rays are emitted in coincidence in $^{11}\text{B}(p, \gamma)$ reaction at $E_p = 163$ keV. Hence, the relative intrinsic efficiency of 11.7 MeV with respect to 4.4 MeV could be measured and was found to be $\sim 24\%$.

4.4 Total Energy Spectrum

The construction of total energy (E_{tot}) spectrum employing the add-back of energy deposited in $\text{LaBr}_3(\text{Ce})$ and $\text{NaI}(\text{Tl})$ crystals was demonstrated by M. Ziębliński *et al.* [14]. The formalism used to construct the E_{tot} in the present case is described in the following. As mentioned earlier, Q_{short} and Q_{long} represent the integrated charge over the short and long time gates, respectively. For a given event, let E_1 and E_2 be the energy deposited in the individual $\text{LaBr}_3(\text{Ce})$ and $\text{NaI}(\text{Tl})$ phosphor elements, respectively and the $q_1(E_1)$ and $q_2(E_2)$ be the corresponding intrinsic charges.

The recorded charges can be represented as

$$Q_{\text{short}} = q_1(E_1)\cos\theta_y + q_2(E_2)\sin\theta_x \quad (4.2)$$

$$Q_{\text{long}} = q_1(E_1)\sin\theta_y + q_2(E_2)\cos\theta_x, \quad (4.3)$$

where θ_x and θ_y represent the tilt angles for pure events in $\text{NaI}(\text{Tl})$ and $\text{LaBr}_3(\text{Ce})$ crystals with respect to Q_{long} and Q_{short} axis, respectively, as shown in Fig. 3. In practice, the tilt angles are defined for the centroid of the $\text{NaI}(\text{Tl})$ and $\text{LaBr}_3(\text{Ce})$ bands. The intrinsic charges can be extracted as

$$q_1(E_1) = k \times (Q_{\text{short}}\cos\theta_x - Q_{\text{long}}\sin\theta_x) \quad (4.4)$$

$$q_2(E_2) = k \times (-Q_{\text{short}}\sin\theta_y + Q_{\text{long}}\cos\theta_y), \quad (4.5)$$

with

$$k = \frac{1}{\cos(\theta_y + \theta_x)}. \quad (4.6)$$

Using gamma rays listed in Table 1 and 2, the calibrations for E_1 vs q_1 and E_2 vs q_2 are obtained. Figure 13 shows the 2D spectrum of E_1 vs E_2 , with $\theta_x = 24^\circ$ and $\theta_y = 45^\circ$ corresponding

to Fig. 3. For each event total energy is obtained as

$$E_{\text{tot}} = E_1 + E_2. \quad (4.7)$$

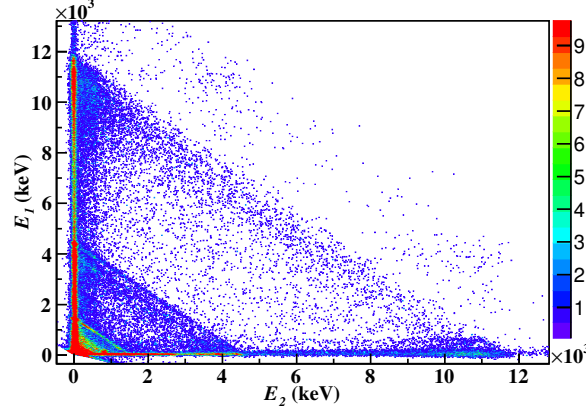


Figure 13. (Color online) Two dimensional spectrum of Fig. 3 after transformation as described in Eq. (4.4)–(4.6) with $\theta_x = 24^\circ$ and $\theta_y = 45^\circ$, for D2 detector with $A1 = 60$ mV.

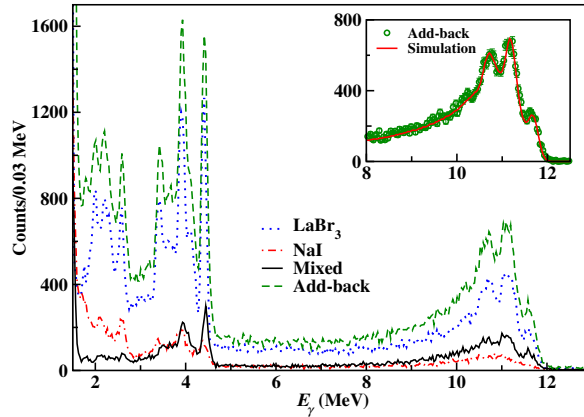


Figure 14. (Color online) The energy spectra of D2 detector in $^{11}\text{B}(p, \gamma)$ reaction at $E_p = 163$ keV for pure $\text{LaBr}_3(\text{Ce})$ events (blue dotted line), pure $\text{NaI}(\text{Tl})$ events (red dash-dotted line) and mixed events (black continuous line). The total energy spectra after add-back (green dashed line) is also shown for comparison. The inset shows a comparison of the experimental and the simulated add-back spectra for $E_\gamma = 11.7$ MeV, where the spectra are normalized to total counts in the range $E_\gamma = 10.4$ to 12.0 MeV.

Figure 14 shows the energy spectra of D2 detector from the $^{11}\text{B}(p, \gamma)$ reaction at $E_p = 163$ keV for pure $\text{LaBr}_3(\text{Ce})$ events, pure $\text{NaI}(\text{Tl})$ events and mixed events. The total energy spectra after add-back (green dashed line) is also shown for comparison, where a significant gain in integral counts due to add-back is evident both at 4.4 MeV and 11.7 MeV. The enhancement factor ($N(E_{\text{tot}})/N(E_1)$) is found to be 1.42 for the 4.4 MeV photo-peak and 1.52 for $E_\gamma = 10.4$ – 12.0 MeV. It can be seen that the counts in $\text{NaI}(\text{Tl})$ are much smaller as compared to the $\text{LaBr}_3(\text{Ce})$ as expected. The simulated add-back spectra were generated following a procedure identical to that of

the data. For each event, total energy is obtained by adding individual energy components after folding in respective resolution function for LaBr₃(Ce) and NaI(Tl) crystals. A comparison of the experimental and the simulated add-back spectra for 11.7 MeV is shown in the inset of Fig. 14, where the spectra are normalized to total counts in the range $E_\gamma = 10.4$ to 12.0 MeV. The excellent agreement is clearly seen. For high energy events, larger fraction of energy is in LaBr₃(Ce) and the add-back spectrum is therefore dominated by LaBr₃(Ce) energy component. In the add-back process the smaller energy component deposited in NaI(Tl) is recovered, resulting in increased counts in second-escape, first-escape and photo-peak as seen in both data and simulations, without any significant effect on the resolution. The energy resolution at 4.4 MeV after add-back is found to be $\sim 3.4\%$ as compared to $\sim 2.9\%$ for LaBr₃(Ce) crystal alone.

5. Summary and Conclusions

Detailed characterization of the individual detector elements (LaBr₃(Ce)-NaI(Tl)) of PARIS detector has been carried out. The detector response is investigated over a wide range of E_γ using radioactive sources and employing $^{11}\text{B}(p, \gamma)$ reaction at $E_p = 163$ keV and $E_p = 7.2$ MeV with CAEN digitizers.

The linearity of energy response of the LaBr₃(Ce) in the phoswich detector is tested upto $E_\gamma = 22.6$ MeV using three different voltage dividers. Stability of high voltage unit is of paramount importance as it can impact the count rate related drifts. The detector gain stability is studied for count rates between 2–220 kHz using B3 type voltage divider (developed by IPHC Strasbourg group for the PARIS detector), for high voltages corresponding to linear energy response upto 22.6 MeV. Detector performance was found to be stable over the count rate 50 to 150 kHz, where the centroid shift and broadening of FWHM at 835 keV is less than 1.5% (11 keV) and 13% (5 keV), respectively. The performance of B3 type voltage divider is found to be very good in terms of resolution, linearity of energy calibration and the count rate handling capability. The stability of the detector gain is found to be better than $\pm 1\%$ over a period of 24 hours.

Time resolution of the phoswich detector is measured with ^{60}Co source after implementing CFD algorithm in the WAVEDUMP acquisition software. The FWHM (digital) $\sim 457 \pm 3$ ps is similar to FWHM (analog) $\sim 454 \pm 6$ ps, at the optimum PMT voltage ($E_{\text{full-scale}} \sim 2$ MeV). The measured time resolution of individual detector FWHM ~ 315 ps, is excellent for neutron- γ separation by TOF measurement at close distances. At lower bias voltages corresponding to linear energy response upto high energy, the time resolution worsens by about 12% (513 ± 3 ps). The energy resolution of $\sim 2.1\%$ at 22.6 MeV is measured for configuration giving the best linearity upto high energy. The optimal configuration corresponding to A1 ~ 60 mV is found to give energy resolution better than 2% at 22.6 MeV and non-linearity of $\sim 10\%$ around 22 MeV. The detector efficiency is measured for $E_\gamma = 0.662 - 4.4$ MeV for three different distances from the face of the detector. The measured efficiency with radioactive sources are in good agreement with GEANT4 based simulations. The relative intrinsic efficiency of LaBr₃(Ce) crystal at 11.7 MeV with respect to that at 4.4 MeV is found to be $\sim 24\%$. The lineshape of high energy gamma rays has been reproduced by GEANT4 based simulation. It is demonstrated that the E_{tot} spectrum with the add-back of individual components of the phoswich detector gives substantial efficiency gain of about 50%, without significantly affecting the resolution. Further, the present measurements indicate that

for the composite signal of the phoswich detector, the digital signal processing with 0.5–1 GHz sampling rate and high resolution (12–14 bit) ADC will be optimal.

Acknowledgments

We thank Mr. K.V. Divekar for assistance during the measurements, Prof. L.C. Tribedi and Mr. Shamik Bhattacharjee for help in the ECR based experiment and Dr. Namita Maiti for the Boron target. We are thankful to the ECR staff and the PLF staff for smooth machine operation during proton beam experiments. The support from PARIS collaboration is gratefully acknowledged.

References

- [1] E. V. D. van Loef *et al.*, *Scintillation properties of LaBr₃:Ce³⁺ crystals: fast, efficient and high-energy-resolution scintillators*, *Nucl. Instr. Meth. A* **486** (2002) 254.
- [2] A. Giaz *et al.*, *Characterization of large volume 3.5'' × 8'' LaBr₃:Ce detectors*, *Nucl. Instr. Meth. A* **729** (2013) 910.
- [3] R. Nicolini *et al.*, *Investigation of the properties of a 1'' × 1'' LaBr₃:Ce scintillator*, *Nucl. Instr. Meth. A* **582** (2007) 554.
- [4] M. Ciemała *et al.*, *Measurements of high-energy γ -rays with LaBr₃:Ce detectors*, *Nucl. Instr. Meth. A* **608** (2009) 76.
- [5] I. Mazumdar *et al.*, *Studying the properties and response of a large volume (946 cm³) LaBr₃:Ce detector with γ -rays up to 22.5 MeV*, *Nucl. Instr. Meth. A* **705** (2013) 85.
- [6] R. Bernabei *et al.*, *Performances and potentialities of a LaCl₃:Ce scintillator*, *Nucl. Instr. Meth. A* **555** (2005) 270.
- [7] R. Billnert *et al.*, *New information on the characteristics of 1 in. × 1 in. cerium bromide scintillation detectors*, *Nucl. Instr. Meth. A* **647** (2011) 94.
- [8] L. M. Fraile *et al.*, *Fast timing study of a CeBr₃ crystal: Time resolution below 120 ps at ⁶⁰Co energies*, *Nucl. Instr. Meth. A* **701** (2013) 235.
- [9] www.crystals.saint-gobain.com/uploadedFiles/SG-Crystals/Documents/BrilLanCe%20380%20Data%20Sheet.pdf
- [10] A. Maj *et al.*, *THE PARIS PROJECT*, *Acta Phys. Polonica B* **40** (2009) 565.
- [11] paris.ifj.edu.pl
- [12] www.hamamatsu.com
- [13] paris.ifj.edu.pl/documents/main/PARIS_status_September_2011_final
- [14] M. Ziębliński *et al.*, *Testing of the PARIS LaBr₃-NaI Phoswich Detector with High Energy Gamma-rays*, *Acta Phys. Polonica B* **44** (2012) 651.
- [15] www.caen.it
- [16] S. Agostinelli *et al.*, *GEANT4 – a simulation toolkit*, *Nucl. Instr. Meth. A* **506** (2003) 250.
- [17] www.tifr.res.in/~abap
- [18] www.tifr.res.in/~pell

- [19] www.nndc.bnl.gov
- [20] F. E. Cecil *et. al.*, *Radiative capture of protons by light nuclei at low energies*, *Nucl. Phys. A* **539** (1992) 75.
- [21] www.tifr.res.in/~pell/lamps.html
- [22] Rene Brun *et. al.*, *ROOT – An object oriented data analysis framework*, *Nucl. Instr. Meth. A* **389** (1997) 81.
- [23] C. Mathieu, S. Kihel, O. Dorvaux, *Private communication, IPHC Strasbourg.*
- [24] Ali Asghar Mowlavi *et. al.*, *Determination of 4.438 MeV γ -ray to neutron emission ratio from a ^{241}Am – ^9Be neutron source*, *Appl. Radiat. Isot.* **60** (2004) 959.
- [25] B. P. Singh *et. al.*, *Relative efficiency of Ge(Li) gamma ray detectors from 0.5 to 12 MeV*, *Nucl. Instr. Meth.* **97** (1971) 475.
- [26] Z. Elekes *et. al.*, *Absolute full-energy peak efficiency calibration of a Clover-BGO detector system*, *Nucl. Instr. Meth.* **503** (2003) 580.
- [27] K.A. Snover *et. al.*, *Radiative proton capture to the ground state and first three excited states of ^{12}C* , *Nuclear Physics A* **285** (1977) 189.
- [28] K.V. Anoop *et. al.*, *Timing of Fast Scintillators using Digitizers*, *Proceedings of the DAE symp. on Nucl. Phys.* **59** (2014) 858.